Data in Brief 42 (2022) 108156

Contents lists available at ScienceDirect

Data in Brief

journal homepage: www.elsevier.com/locate/dib

Data Article

Experimental image dataset for validation of the noise-induced bias that affects Digital Image Correlation

Antonio Baldi*, Pietro Maria Santucci, Filippo Bertolino

Dipartimento di Ingegneria Meccanica, Chimica e dei Materiali, Universitá degli Studi di Cagliari, Via Marengo 2, Cagliari, Italy

ARTICLE INFO

Article history:
Received 10 March 2022
Revised 3 April 2022
Accepted 4 April 2022
Available online 10 April 2022

Dataset link: Experimental image dataset for validation of the noise-induced bias that affects Digital Image Correlation (Original data)

Keywords:
Digital Image Correlation
Noise-Induced Bias
High Precision Positioning
Interferometric Measurement

ABSTRACT

The present article shares with the scientific community several image sets used for experimentally validating the noise-induced bias on different Digital Image Correlation (DIC) formulations, as reported in Baldi et al. [1]. These sets are provided with a description of the experimental setup used for image acquisition. The basic idea is to acquire a series of images obtained by rigidly translating the target, where incremental displacement is of the order of a small fraction of a pixel. This condition requires a high-precision control of the target position through the tests. Moreover, the noise content of each image set is modulated using a statistical approach that uncouples the intensity field from the standard deviation. Lastly, the images are acquired with different exposure conditions to analyze the gray tone gradient effect on noise-induced bias.

DOI of original article: 10.1016/j.optlaseng.2022.107012

* Corresponding author.
E-mail addresses: antonio.baldi@unica.it, antonio.baldi@dimcm.unica.it (A. Baldi).

https://doi.org/10.1016/j.dib.2022.108156

Specifications Table

Subject	Mechanical Engineering
Specific subject area	Experimental Mechanics (Digital Image Correlation).
Type of data	Monochromatic Images, Text Files
How the data were acquired	Data were acquired using an Allied Vision Pike 421B monochromatic digital camera (maximum resolution 2048 × 2048 pixels); The experimental set-up was composed by: • An in-house-developed monolithic X-Y stage, operated by two Thorlabs PZS001 Piezo stack actuators with strain gauge. • A strain gauges signal conditioner HBM Quantum-X 840. • A Twyman-Green interferometer with a He-Ne laser (wavelength = 632.8 nm). • A National Instrument NI-6229 DAQ board. • A two-channel piezo amplifier (assembled using two Physik Instrumente E-836 OEM modules).
Data format	Raw
Description of data collection	Data consists of three sets of images sampled with different exposure times. Each one contains 46 images acquired during a rigid body translation test. Depending on the set, each image results from the average of one, two, four, or eight shots.
Data source location	• Institution: Università degli Studi di Cagliari • City/Town/Region: Cagliari/Cagliari/Sardinia • Country: Italy
Data accessibility	Repository name: Mendeley Data Data identification number: DOI data: 10.17632/2423jdt345.1 Direct URL to data: https://data.mendeley.com/datasets/2423jdt345/1
Related research article	A. Baldi, P.M. Santucci, F. Bertolino, *Experimental Assessment of Noise Robustness of the Forward-Additive, Symmetric-Additive and the Inverse-Compositional Gauss-Newton Algorithm in Digital Image Correlation*, Optics and Lasers in Engineering. 154 (2022) 107012 https://doi.org/10.1016/j.optlaseng.2022.107012.

Value of the Data

- Digital Image Correlation (DIC) is a widespread optical technique used to measure in-plane, tri-dimensional and volumetric motion [2]. The DIC technique assumes that the single-pixel intensity never changes during motion (i.e., the optical flow remains constant). Although, this statement is never fully satisfied because of the interference of several external and internal noise sources.
  Furthermore, the interpolation used to evaluate pixel intensity at non-integer locations has been widely addressed as a source of bias [3]. Wang et al. [4,5] take into account also the effect of the noise on the interpolation bias, while Wang et al. [6] propose a formulation for modeling the expectation of the measured displacement in terms of interpolation and noise-induced effects.
- From the experimental side, the data support the acknowledgment of the noise bias that affects several DIC formulations. Because the maximum gray gradient is limited by the maximum allowed intensity, by providing similar tests with progressively decreasing maximum gray value, the data allow the analysis of the influence of gradient on noise bias. Moreover, because each intensity value was acquired at multiple noise levels (because of the averaging of the images), the influence of noise can also be evaluated.
  Apart from noise induced-bias, data allow for evaluation of polynomial-induced bias because the true motion is accurately provided, thus giving a reference value to compare with.
- The image sets can be useful to all scientist working on DIC formulation and, in general, to scientist working on DIC code response to noise bias. Moreover, it can be used to verify the accuracy and reliability of newly developed codes, because it provides experimental images acquired in very different conditions whose displacement is accurately known.
- Data can be used to validate from the experimental side DIC formulations and to test the various interpolating techniques used in DIC codes.

1. Data Description

The data source is organized in three directories, named “1000”, “200” and “50” which refers to the exposure time. Thus, images in the last directory are twenty times darker than those in the first one and appear mostly black if the intensity is not equalized.

In each primary directory, there are four sub-folders, named “x1”, “x2”, “x4”, “x8”, containing images obtained by averaging the intensity fields of one, two, four, or eight shots. Each image is a 1600×1200 (width $\times$ height) 8-bits monochromatic raw file[1], stored as a byte stream in row-major order. No header or metadata is present.

In each sub-folder, there are 46 images (in binary format; file extension: `.bin`) acquired during the rigid body motion of the specimen and two text files[2] reporting the horizontal translation motion in micrometers (file extension: `.um`) and in pixels (file extension: `.px`). The various experiments have been performed using nominally identical translation steps, but the actual positions of image acquisition differ slightly. The location of image 0 (assumed at the origin) is not reported in the text file. Note that also image 1 is roughly at $x = 0$. This choice allows for using the same numerical processing technique in data.

Fig. 1 shows the set-up used to provide the sub-pixel motion. In particular, Fig. 1a furnishes an overview of both the X-Y stage and the Michelson interferometer. In contrast, Fig. 1b focus on the design of the X-Y stage itself.

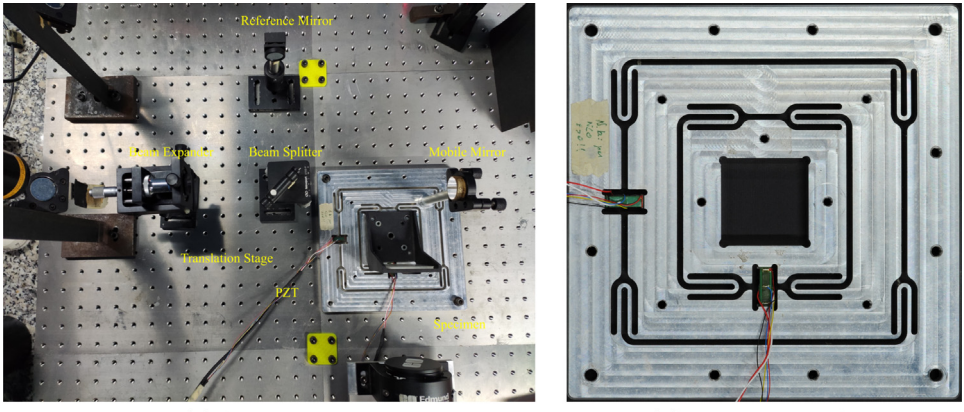

(a) *Set-up overview.* (b) *X-Y Monolithic Stage.*

Fig. 1. Experimental set-up design: (a) Overview of the entire measurement system; (b) Particular of the home-made X-Y translational stage and its Piezo actuators.

Fig. 2 describes the schematic of the whole set-up and focuses on the configuration of the Michelson interferometer.

[1] Images can be viewed using the public domain utility ImageJ by selecting `File/Import/Raw...` and settings the appropriate parameters (Image type: 8-bit, Width: 1600 pixels, Height: 1200 pixels).

[2] The text files are single column and uses Unix-style end of line LF character (ASCII `0x0A`).

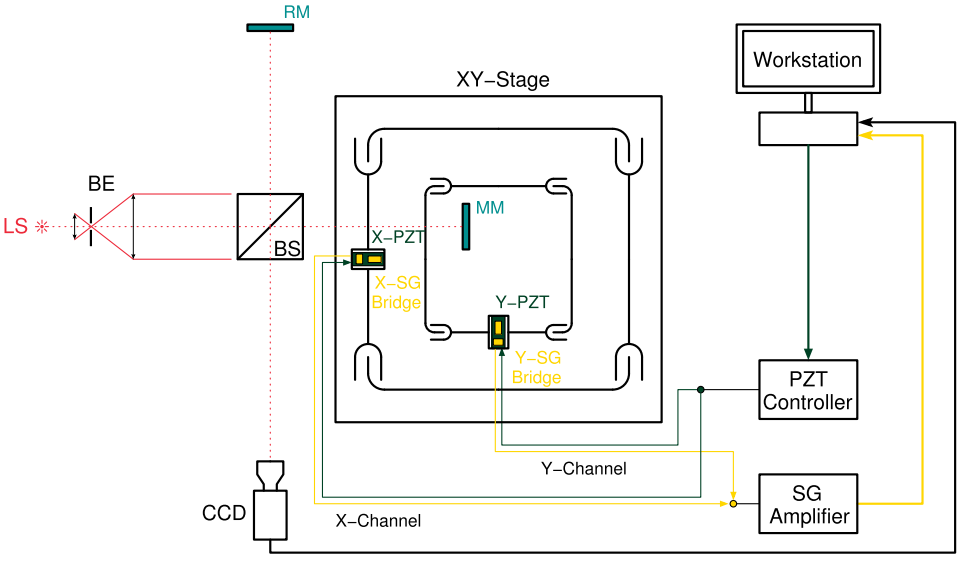

Fig. 2. Schematic of Michelson Interferometer. BE: beam expander; BS: beam splitter; LS: laser source; PZT: piezo translator; SG: strain gauge; RM: reference (fixed) mirror; MM: mobile mirror.

Fig. 3 refers to the dynamical response of the AVT Pike F412b: Fig. 3a shows the Signal-to-Noise Ratio with respect to the gray level, and Fig. 3b graphs the Standard Deviation trend at the same abscissa of the former. The effect of using a single shot or the sum of 2, 4, or 8 frames is also taken into account. All the data are expressed in terms of normalized intensity.

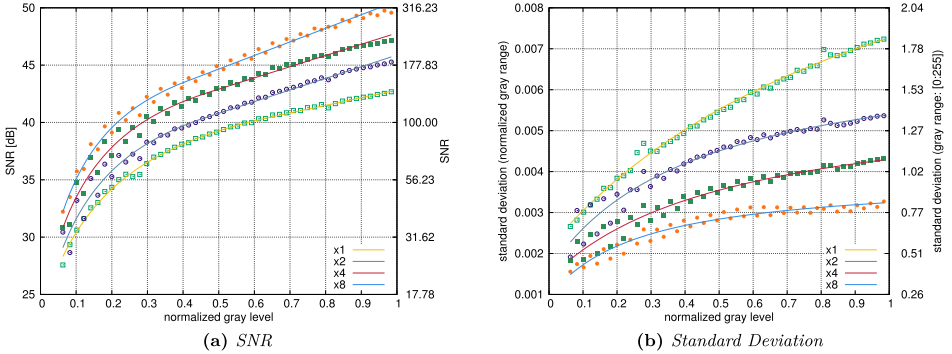

(a) *SNR* (b) *Standard Deviation*

Fig. 3. Dynamic response of Pike F421b camera in terms of SNR and standard deviation for multi-acquisition procedure [1].

2. Experimental Design, Materials and Methods

The experimental setup was designed to test the noise effect on several DIC formulations. In particular, the experiments were able to show:

1. The influence of the gray gradient (spatial gradient of image intensity).
2. The influence of the standard deviation of image intensity.

A high-precision (2-axes) motion system was designed and built to accomplish these targets. The translation stage is able of sub-micron accuracy, which, combined with a high-resolution digital camera, allows for sub-pixel resolution.

2.1. Experimental hardware

The images are acquired using an Allied Vision Pike F421b monochromatic camera [7], with a 2048×2048 resolution and a $0.9\times$ Edmund Optics Large Format Telecentric lens. The image quantization is set to 8 bits to avoid any problem with multi-byte integer representation (Endianness). The CCD nominal pixel size is 7.4 µm, but, taking into account the lens magnification, the actual translation range needed to cover a single pixel is about 8.2 µm.

During the experiment, a target, sprayed with a speckle pattern and fixed through an L support to the X-Y stage (Fig. 1a), was imaged during motion. At the same time, the acquisition location was monitored.

The translation system consists of a monolithic aluminum alloy plate, shown in Fig. 1b, actuated by two PZS001 piezoelectric stack devices produced by Thorlabs [8], each equipped with full-bridge strain gauges sensitive to longitudinal strain.

Because piezoelectric actuators are pretty nonlinear, a closed loop control is implemented to achieve a high-precision positioning. The strain gauges monitor the stage position, whose signals are conditioned through an HBM QuantumX 840 amplifier [9]. The system was calibrated through a Michelson interferometer, as shown in Fig. 1a, while a more detailed schematic is proposed in Fig. 2.

The source is a HeNe laser with a wavelength of 632.8 nm. The mobile mirror (MM, Fig. 2) is fixed to the X-Y stage to perform a displacement measurement by analyzing the acquired intensity history. Indeed, the interferometric fringe pattern is imaged by another camera (Basler A641f with 1600×1200 resolution). The integration of the acquired fringe pattern results in a sinusoidal signal controlled by the phase-variation imposed through mobile mirror shifting. The stage motion is slow enough to consider maximum and minimum fringe intensities constant through measurement. Indeed, once the mean intensity and modulation are known, the phase can be computed.

The post-processing technique uses the Empirical Mode Decomposition [10] to extract the principal mode and the mono dimensional Hilbert transform to compute the quadrature signal. The last steps are the computation of phase modulo 2π throughout the inverse tangent of the two signals and the phase unwrapping [11]. By scaling the phase by $\lambda/2\pi$, this procedure leads to the computation of displacements.

Assuming that the interferometric set-up is able to resolve one-hundredth of a fringe, the resolution in terms of distance might be evaluated in 3.16 nm. This value, expressed in terms of pixels, gives the experimental set-up a resolution of $3.16\ \text{nm}/8200\ \text{nm/pixel} = 4 \times 10^{-4}$ pixels. The strain gauge resolution is estimated at[3] 5.5×10^{-4} pixels.

[3] The mounting configuration of strain gauges on PZS001 is a standard configuration for tensile stress using two active and two dummy strain gauges, so the measured deformation is doubled with respect to the actual one. Indeed, the deformation required to cover a pixel can be estimated as:

$$2\frac{\overbrace{8.2\ \mu\text{m}}^{\text{Pixel Size}}}{\underbrace{9\times10^{-3}\ m}_{\text{Strain Gauge Reference Length}}} = 1822\ \mu\text{m/m}$$

By computing the inverse of the latter, we obtain the resolution in terms of $\mu\varepsilon$/pixel.

2.2. Experimental Methodology

The first step to investigate the gradient effect is the camera calibration in terms of response to noise. To this end, one hundred nominally identical images have been acquired. By assuming that each pixel's "true" gray level can be found in the mean image, the pixels can be classified and the *Signal-to-Noise Ratio* (SNR) estimated.

Fig. 3b shows that the standard deviation roughly doubles when moving from dark to maximum intensity. On the contrary, the maximum gray gradient (limited by the maximum gray level[4]) increases by two orders of magnitude. Because noise-induced bias is controlled by the ratio of the standard deviation and the gradient of grays, the noise-induced bias decreases with mean image intensity.

Indeed, by reducing the mean image intensity, it is possible to investigate the contribution of noise to bias due to gradient. The procedure consists of acquiring several images sets, obtained by target translation, with decreasing exposure time. The choice of reducing the shutter time instead of modifying the flux of the illumination system provides for a stable temperature distribution over the whole experiment time. Each set comprises 46 images obtained by a relative displacement of 0.2 μm to cover a total range of about one pixel.

To evaluate the dependence of noise-induced bias from the standard deviation of the intensity, the described acquisition procedure must be modified. Indeed, by summing the intensity field of two images, the resultant intensity field is doubled while its noise content is scaled by $\sqrt{2}$. Following this idea, dividing by two the result leads to an image with the same intensity pattern as the analogous one-shot but with a scaled standard deviation. Fig. 3 shows the effect of this procedure on the SNR and the standard deviation for a sample acquired with a single-shot frame and as a result of two, four, and eight shots.

This "multi-sampling" technique provides sets of images with a nominally identical intensity gradient but different standard deviation: this is a remarkable advance because it consents to analyze the noise-induced effects of standard deviation independently from intensity gradient. The latter one can be modulated by controlling the image's mean intensity.

The sets of images are acquired by the same translation test described before. However, the images result from summing two, four, or eight single-shot intensities for each acquisition step, respectively divided by two, four, and eight.

2.3. Post processing

The images have been stored in binary form as acquired: no filtering or resizing has been performed. The only modification is setting the first byte of each data stream to `0xFF`: in this way, the maximum intensity of each image is always the same, irrespectively of the mean gray value, thus preventing automatic intensity equalization of our DIC code.

Pixel size has to be known to compute the displacements in pixels (stored in files with extension `.px` in each folder). The exact value is difficult to estimate because it depends on slight misalignments of the camera (in principle optical axis should be orthogonal to the displacement direction), the precision of the optical components, and testing temperature (which may slightly differ from test to test). To solve this problem, we opted for a software approach. Because polynomial bias is null at integer displacements irrespectively of the used interpolating polynomial, it suffices to analyze the displacement history using different formulations for gray tones interpolation; the point where all the displacement histories cross flags the pixel size. Using this approach, we identified the experimental pixel size, which results in 8.23 μm in almost all our tests.

[4] The nominal range of the image gradient, expressed in terms of normalized intensity, extends from $\frac{1}{2^l-1}$ to 1, where l is the bits number used in the image quantization.

Declaration of Competing Interest

The authors declare that they have no known competing financial interests or personal relationships that could have appeared to influence the work reported in this paper.

Data Availability

Experimental image dataset for validation of the noise-induced bias that affects Digital Image Correlation (Original data) (Mendeley Data).

CRediT Author Statement

Antonio Baldi: Conceptualization, Methodology, Software, Visualization, Investigation, Formal analysis, Writing – original draft; **Pietro Maria Santucci:** Writing – original draft, Investigation; **Filippo Bertolino:** Validation.

Acknowledgments

The authors wish to thank Mr. Gianluca Marongiu and Mr. Daniele Lai for their support in the development of the experimental set-up.

References

[1] A. Baldi, P. Santucci, F. Bertolino, Experimental assessment of noise robustness of the forward-additive, symmetric-additive and the inverse-compositional gauss-newton algorithm in digital image correlation, Opt. Lasers Eng. 154 (2022) 107012, doi:10.1016/j.optlaseng.2022.107012.
[2] M.A. Sutton, J.J. Orteu, H. Schreier, Image Correlation for Shape, Motion and Deformation Measurements: Basic Concepts, Theory and Applications, Springer Science & Business Media, 2009.
[3] H.W. Schreier, J.R. Braasch, M.A. Sutton, Systematic errors in digital image correlation caused by intensity interpolation, Opt. Eng. 39 (2000) 2915–2921, doi:10.1117/1.1314593.
[4] Z. Wang, H. Li, J. Tong, J. Ruan, Statistical analysis of the effect of intensity pattern noise on the displacement measurement precision of digital image correlation using self-correlated images, Exp. Mech. 47 (2007) 701–707, doi:10.1007/s11340-006-9005-9.
[5] Y. Wang, P. Lava, P. Reu, D. Debruyne, Theoretical analysis on the measurement errors of local 2D dic: part i temporal and spatial uncertainty quantification of displacement measurements, Strain 52 (2016) 110–128, doi:10.1111/str.12173.
[6] Y. Wang, M. Sutton, H. Bruck, H. Schreier, Quantitative error assessment in pattern matching: effects of intensity pattern noise, interpolation, strain and image contrast on motion measurements, Strain 45 (2009) 160–178, doi:10.1111/j.1475-1305.2008.00592.x.
[7] Allied Vision, PIKE 421b technical manual, 2018. https://cdn.alliedvision.com/fileadmin/content/documents/products/cameras/Pike/techman/Pike_TechMan_01.pdf.
[8] Thorlabs Inc., PZS01 technical manual, 2015. https://www.thorlabs.com/thorproduct.cfm?partnumber=PZS001.
[9] HBM, HBM quantumx 840 technical manual, 2012. https://www.hbm.com/en/2129/quantumx-mx840b-8-channel-universal-amplifier/.
[10] A. Baldi, S. Equis, P. Jacquot, Phase extraction in dynamic speckle interferometry by empirical mode decomposition, in: Experimental Analysis of Nano and Engineering Materials and Structures, Springer, 2007, pp. 719–720, doi:10.1007/978-1-4020-6239-1_357.
[11] A. Baldi, Phase unwrapping by region growing, Appl. Opt. 42 (2003) 2498–2505, doi:10.1364/AO.42.002498.